

Published in final edited form as:

*Int J Cancer*. 2014 June 1; 134(11): 2633–2645. doi:10.1002/ijc.28590.

## Origin and pharmacological modulation of tumor-associated regulatory dendritic cells

Hua Zhong<sup>1</sup>, Dmitriy W. Gutkin<sup>2</sup>, Baohui Han<sup>1</sup>, Yang Ma<sup>2</sup>, Anton A. Keskinov<sup>2</sup>, Michael R. Shurin<sup>2,3</sup>, and Galina V. Shurin<sup>1,2</sup>

<sup>1</sup>Department of Pulmonary Disease, Shanghai Chest Hospital, Shanghai Jiaotong University, Shanghai, China

<sup>2</sup>Department of Pathology, University of Pittsburgh Medical Center, Pittsburgh, PA

<sup>3</sup>Department of Immunology, University of Pittsburgh Medical Center, Pittsburgh, PA

### Abstract

Protumorigenic activity of immune regulatory cells has been proven to play a major role in precluding immunosurveillance and limiting the efficacy of anticancer therapies. Although several approaches have been offered to deplete myeloid-derived suppressor cells (MDSC) and regulatory T cells, there are no data on how to control suppressive dendritic cell (DC) accumulation or function in the tumor environment. Although immunosuppressive function of DC in cancer was implicated to immature and plasmacytoid DC, details of how conventional DC (cDC) develop immunosuppressive properties remain less understood. Here, we show that the development of lung cancer in mice was associated with fast accumulation of regulatory DC (regDC) prior to the appearance of MDSC. Using the *in vitro* and *in vivo* approaches, we demonstrated that (i) both cDC and MDSC could be polarized into protumor regDC in the lung cancer environment; (ii) cDC → regDC polarization was mediated by the small Rho GTPase signaling, which could be controlled by noncytotoxic doses of paclitaxel; and (iii) prevention of regDC appearance increased the antitumor potential of DC vaccine in lung cancer. These findings not only bring new players to the family of myeloid regulatory cells and provide new targets for cancer therapy, but offer novel insights into the immunomodulatory capacity of chemotherapeutic agents used in low, noncytotoxic doses.

### Keywords

tumor microenvironment; dendritic cells; MDSC; small Rho GTPases; taxol

---

Tumors develop in the complex tissue microenvironment in the presence of different immune cells, which can mediate stimulatory and inhibitory pressure on the proliferative, angiogenic, metastasizing and immunomodulatory properties of malignant cells.<sup>1–3</sup> Several

---

© 2013 UICC

**Correspondence to:** Galina V. Shurin, Department of Pathology, University of Pittsburgh Medical Center, Scaife Hall S733, 3550, Terrace Street, Pittsburgh, PA 15261, USA, Tel.: +412-648-9831, Fax: +412-648-8158, shuringv@upmc.edu.

Additional Supporting Information may be found in the online version of this article.

subsets of immune regulatory cells are recruited to the tumor microenvironment, where they support tumor progression, protect the tumor from host immunity and foster therapeutic resistance.<sup>4,5</sup> The contribution of tumor-associated M2 macrophages and N2 neutrophils, myeloid-derived suppressor cells (MDSC), regulatory lymphocytes and mast cells to tumor development and progression is increasingly well understood,<sup>6</sup> as are the reciprocal communications with neoplastic cells that mediate their recruitment and activation.<sup>7,8</sup> Recently, a new player has been added to the family of myeloid regulatory cells—regulatory dendritic cells (regDC).<sup>9</sup> The fundamental role for conventional DC (cDC) as preeminent antigen-presenting cells in the induction of immune responses is well accepted. However, emerging studies have highlighted the role played by the microenvironment in re-programming DC to a tolerogenic state.<sup>10</sup>

The role of tolerogenic DC in transplantation, allergy, autoimmune and infectious diseases has been well documented and the term “regDC” has been ascribed to cells with different phenotypes and functions. For instance, regDC were characterized as DC expressing high levels of MHC and low levels of costimulatory molecules; cells with high CD80 and CD86 expression; cells with low CD40, CD80, CD86 and MHC class II expression; or DC with low expression of MHCII and CD86 and high levels of CD80 and CD40. RegDC were also described as cells producing or not producing IL-10 or nitric oxide, or TGF- $\beta$ , or COX-2, or indoleamine 2,3-dioxygenase and cells inducing or not inducing regulatory T (Treg) cells.<sup>11</sup> The nature of regDC in cancer is less well understood, with the exception of plasmacytoid DC.<sup>12,13</sup> Much less is known about “conventional” regDC in cancer, and only a few reports suggest that MHCII<sup>+</sup>CD11b<sup>+</sup>CD11c<sup>+</sup>tumor-infiltrating DC may act as regDC to suppress CD8<sup>+</sup>T cells.<sup>14,15</sup> However, their contributory functions to tumor development and progression, as well as their origin *in vivo*, the mechanisms of polarization and an opportunity to harness, have not been yet investigated.

Here, we report that in the lung cancer, cDC and MDSC can be converted into Gr-1<sup>neg</sup> or Gr-1<sup>pos</sup> regDC, with potent protumorigenic and immunosuppressive properties, *in vivo*. Addition of noncytotoxic doses of paclitaxel attenuated tumor-mediated propagation of regDC *in vivo* and *in vitro* and augmented the therapeutic efficacy of DC vaccines. These data provide new insights into the immunobiology of tumor-associated regDC and offer proof-of-principle of the practicality of combining an anti-regDC approach with cancer immunotherapy.

## Material

### Mice

A 6 to 8-week-old male C57BL/6 (Taconic), C57BL/10ScNJ TLR4<sup>-/-</sup> mice and B6.FVB-Tg (Itgax-DTR/EGFP) 57Lan/J CD11c-DTR transgenic mice (Jackson Laboratories) were housed in a pathogen-free facility under controlled temperature, humidity and light.

### Animal models and experimental designs

Immune regulatory cells were evaluated in the lymphoid and nonlymphoid tissues using the intravenous ( $1 \times 10^5/300 \mu\text{l}$  PBS) 3LL lung cancer and B16 melanoma lung metastasis

models. Animals were sacrificed 1, 2 and 3 weeks post-tumor inoculation, and single cell suspensions from the lung and spleen specimens were prepared using collagenase D (1% w/v, Sigma) and the gentle MACS dissociator (Milteyi Biotec). Bone marrow cells were flushed from tibia. All cell suspensions were analyzed for the presence of MDSC, Treg, regDC and cDC by flow cytometry.

To evaluate the protumorigenic potential of regDC *in vivo*, mice were injected i.v. with 1/10 of the minimum tumorigenic dose of 3LL cells ( $1 \times 10^4$  cells). FACS sorted CD11c<sup>low</sup>CD11b<sup>high</sup>GR-1<sup>neg</sup> regDC or CD11c<sup>high</sup>CD11b<sup>low/neg</sup> GR-1<sup>neg</sup> cDC from TCM-treated DC cultures were injected ( $5 \times 10^5$  cells, i.p.) in mice on D3 and D10 after inoculation of tumor cells. After 10 days, animals were sacrificed; lungs were removed, fixed and used for H&E staining for detection of macro and microtumor nodules. To evaluate the immunosuppressive potential of regDC *in vivo*, mice received i.v. injection of  $1 \times 10^5$  (minimum tumorigenic dose) 3LL cells followed by i.p. injection of  $5 \times 10^5$  regDC or cDC cells as above. After 10 days, macro- and micro-metastases were determined.

To establish whether low, noncytotoxic doses of paclitaxel (Taxol) alter formation of regDC in tumor-bearing mice, animals received i.v. inoculation of 3LL cells ( $1 \times 10^5$ ). Paclitaxel was administered on D5 and D10 (1 mg/kg, i.p.). Spleens and lungs were harvested on D14 for the analysis of DC subsets. Similar experiments were scheduled using C57BL/10ScNJ TLR4<sup>-/-</sup> mice to determine whether the effect of paclitaxel on regDC formation is mediated by TLR4 signaling. To confirm that administration of 1 mg/kg paclitaxel devoted the cytotoxic and cytostatic effects, mice bearing  $\sim 5 \times 5$  mm<sup>2</sup> s.c. tumors received single injection of saline, 15 mg/kg ( $\sim 3/4$  MTD, maximum tolerated dose) and 1 mg/kg paclitaxel (1/20 MTD). 48 hr later, tumors were harvested, fixed and used for the analysis of tumor cell apoptosis and proliferation using TUNEL and Ki67 staining.

To evaluate whether prevention of regDC formation with paclitaxel suppresses tumor progression, different therapeutic schedules were applied. Mice received 3LL cells ( $1 \times 10^5$ , i.v., D0). Paclitaxel (1 mg/kg, i.p.) was administered on D6, D11 and D16. Nonpulsed bone marrow-derived DC ( $1 \times 10^6$ , i.p.) were injected on D12 and D17 with and w/o paclitaxel. Animals were sacrificed on D21. The presence of tumor nodules in the lungs was assessed visually and by light microscopy after H&E staining. Survival of animals was also determined.

CD11c-DTR transgenic mice (B6.FVB-Tg(Itgax-DTR/EGFP)57Lan/J) were used to test the biological significance of regDC depletion *in vivo* prior to cDC vaccine. ITgax-DTR mice were injected i.v. with  $1 \times 10^5$  3LL cells. After 5 days, mice were treated with either PBS (control), paclitaxel (1 mg/kg, i.p.  $\times 2$ ) 2 days prior to DC ( $1 \times 10^6$ , i.p.) vaccine, or i.p. diphtheria toxin (DT) (2 ng/g  $\times 2$ ) 2 days prior to DC vaccine. Lungs were harvested on D21 and analyzed for the presence of tumor nodules. Tumor-specific IFN- $\gamma$  producing CTL were also determined.

For histopathology, specimens were fixed in PFA and embedded in paraffin. H&E stained slides were reviewed on an Olympus BX45 microscope with UPlanFLN 10 $\times$ /0.30 objective, Spot Insite 2Mp CCD camera.

All animal experiments included 6–7 mice per group and were repeated at least 2–3 times.

### Statistical analysis

For a single comparison of two groups, the Students' *t* test was used after evaluation of normality. If data distribution was not normal, a Mann–Whitney rank sum test was performed. For the comparison of multiple groups, analysis of variance was applied. For all statistical analyses,  $p < 0.05$  was considered significant. All experiments were repeated at least two times. Data are presented as the mean  $\pm$  SEM. Please see Supporting Information for all experimental procedures.

## Results

### Tumor development is associated with emergence of regulatory DC *in vivo*

One of the key problems in determining the biological significance of immunosuppressive tumor-associated DC *in vivo* is the absence of a model system that allows their characterization in the absence other regulatory cells, first of all, MDSC and Treg. Therefore, we evaluated several animal tumor models for the presence of MDSC, Treg and regDC. Our results revealed gradual and differential appearance of immune regulatory cells in the lymphoid tissues and the tumor microenvironment. Figure 1a shows that orthotopic growth of lung carcinoma was associated with significant elevation of CD11b<sup>+</sup>GR-1<sup>+</sup>MDSC in the spleen (up to 5-fold,  $p < 0.05$ ) and the lung tumor microenvironment (up to 2.5-fold,  $p < 0.05$ ) only at week 3 after tumor cell inoculation. The levels of CD4<sup>+</sup>CD25<sup>+</sup>FoxP3<sup>+</sup>Tregs were not changed (Fig. 1a). However, the dynamics of regDC emergence was different: CD11c<sup>low</sup>CD11b<sup>high</sup> regDC were increased systemically and in the tumor microenvironment starting from the first week after tumor cell injection and were gradually and significantly elevated during the second and third weeks (Fig. 1a). Tumor-associated regDC were CD103<sup>+</sup> and CD205<sup>low</sup>, expressed low levels of MHCII, CD86 and CD40, did not express macrophage marker F4/80 and were up to 50% Ly6C, Ly6G positive (Fig. 1b). Splenic regDC displayed a similar phenotype. These results demonstrate that, in the 3LL lung metastasis model, appearance of regDC *in vivo* precedes emergence of MDSC, which allows the studying of regDC *in vivo* 2 weeks after the tumor cell injection without interference from MDSC. Importantly, the appearance of regDC in the lungs was accompanied by a significant decrease (8- to 10-fold,  $p < 0.05$ ) of conventional CD11c<sup>high</sup>CD11b<sup>low/neg</sup> CD205<sup>high</sup>CD103<sup>+</sup>cDC (Figs. 1a and 1b). Similar significant downregulation of cDC was observed in the spleens of tumor-bearing mice (Fig. 1a).

Differential emergence of MDSC and regDC in the 3LL model raised a question about the tumor specificity of this new phenomenon. To test this, we applied a similar experimental design to the B16 melanoma lung metastasis model. The summary of these studies are shown in Table 1 (Supporting Information), which suggests that there are several significant differences between regulatory cell subsets in mice receiving B16 or 3LL cells. First, B16 cells induced higher levels and earlier appearance of MDSC in the lungs. Second, B16 cells induced lower levels of regDC in the lungs and spleens. Third, B16, unlike 3LL cells, induced upregulation of Tregs in the spleen. Thus, systemic administration of 3LL resulted in fast recruitment of regDC to the lungs and spleens during the first 2 weeks of tumor

development without interference with other regulatory cells. This suggests that *i.v.* administration of 3LL cells represents a feasible model to study regDC *in vivo* without an interference with MDSC and Tregs.

To prove that tumor-associated regDC are functionally active, we tested their ability to inhibit proliferation of activated T cells. CD11c<sup>low</sup>CD11b<sup>high</sup> regDC were sorted from the lung tumor tissues harvested 2 weeks after mice were injected with 3LL cells, and then mixed with preactivated T cells. Figure 1d shows that regDC significantly inhibited T cell proliferation (>2-fold,  $p < 0.05$ ), while cDC (bone marrow-derived or splenic CD11c<sup>+</sup>DC from tumor-free mice) upregulated proliferation of T cells. Thus, the development of lung cancer was associated with fast and significant accumulation of immunosuppressive regDC in the lymphoid tissues and the lung tumor microenvironment. This raises the next question about the opportunity to generate regDC in the *in vitro* model system for their detailed analysis.

### Conventional DC are polarized into regDC in the tumor microenvironment *in vitro* and *ex vivo*. Phenotype and functional analyses

We tested the hypothesis that bone marrow-derived cDC could be polarized into immunosuppressive regDC in the lung cancer microenvironment *in vitro*. Figure 1c shows that the addition of 3LL-TCM to D5 semimature DC resulted in conversion of a subset of the CD11c<sup>high</sup>CD11b<sup>low/neg</sup> cDC to CD11c<sup>low</sup>CD11b<sup>high</sup> regDC. The levels of regDC increased from  $1.5 \pm 0.2\%$  in control cultures to  $9.8 \pm 0.6\%$  in cultures exposed to TCM ( $p < 0.05$ ,  $N=7$ ). In the same cultures, the population of cDC in the cultures treated with 3LL-TCM decreased by four- to fivefold ( $p < 0.05$ ) (Fig. 2c). Interestingly, regDC polarized from bone marrow-derived cDC under the influence of 3LL-TCM did not express GR-1 molecules (Fig. 2c).

Recent findings demonstrated that the transcriptional regulator *Foxo3* plays a critical role in tolerogenic function of plasmacytoid DC in prostate cancer.<sup>16</sup> Although regDC in our model system did not express the pDC marker PDCA1, we assessed *Foxo3* expression in regDC in the lung cancer model. Flow cytometry analysis of *in vitro*-generated regDC, as well as regDC from spleens and lungs of 3LL-bearing mice, revealed that they do not express FOXO3 protein.

As these data demonstrated cDC  $\rightarrow$  regDC polarization *in vitro*, we next tested the immunosuppressive potential of regDC. As shown in Figure 1d, sorted regDC generated *in vitro* had a similar ability to suppress T cell proliferation as regDC sorted from tumor-bearing mice. Therefore, the next question was whether *in vitro*-produced regDC might represent a subset of immature DC (imDC) (based on regDC phenotype), which may display the tolerogenic property in certain conditions *in vivo*. We therefore demonstrated that imDC prepared in DC cultures did not block proliferation of preactivated T cells (Fig. 2e). Thus, these data (i) suggest that in the *in vitro* tumor microenvironment, cDC can be polarized into immunosuppressive regDC and (ii) raise the next question of whether cDC can be converted into regDC *in vivo*.

To demonstrate that cDC  $\rightarrow$  regDC polarization can take place *in vivo*, we isolated CD11c<sup>high</sup>CD11b<sup>low/neg</sup> cDC by FACS from the lungs of tumor-free mice (Fig. 2a) and coincubated them with 3LL cells for 72 hr. The flow cytometry analysis revealed that, in the presence of tumor cells, cDC polarized into regDC, which were GR-1<sup>neg</sup> and suppressed proliferation of preactivated T cells (>4-fold,  $p < 0.05$ ) (Figs. 2b and 2c). However, ~50% of regDC in the tumor microenvironment *in vivo* were GR-1<sup>+</sup> (Fig. 1b). Therefore, we sorted MDSC from the lungs of tumor-free mice (Fig. 2a) and co-incubated them with tumor cells. The results revealed that MDSC could be polarized into regDC *ex vivo*: the level of regDC was up to eightfold higher than the one in control cultures ( $p < 0.05$ ; Fig. 2d). The functional assay confirmed the immunosuppressive potential of MDSC-derived regDC (Fig. 2e). For direct demonstration of MDSC  $\rightarrow$  regDC differentiation *in vivo*, bone marrow-derived MDSC were labeled with CFDA SE and injected in 3LL-bearing mice. Analysis of “green” regDC 3–5 days later revealed that up to 25% of regDC in the lungs and up to 10% of regDC in the spleen were CFDA SE positive (data not shown). This suggests that MDSC can differentiate into regDC *in vivo* in tumor-bearing mice.

These results explain the appearance of both Gr-1<sup>+</sup> and GR-1<sup>neg</sup> regDC in the tumor microenvironment *in vivo*. They also confirm that, in the tumor-free conditions, MDSC differentiate into immature and mature cDC, which loose expression of GR-1 (Fig. 2d). Together, these data not only demonstrate tumor-induced emergence of regDC in the tumor environment, but also prove that both cDC and MDSC can be polarized into functional regDC *in vitro* and *in vivo*. The data raise the next question about the biological significance of regDC in cancer.

### Protumorigenic properties of regDC *in vivo*

We next tested whether regDC may support tumor growth *in vivo*. DC cultures were treated with 3LL-TCM to generate regDC, which are Gr-1<sup>neg</sup>. CD11c<sup>low</sup>CD11b<sup>high</sup> regDC and CD11c<sup>high</sup>CD11b<sup>low/neg</sup> cDC subsets were isolated by FACS and injected into mice inoculated with 1/10 of the minimum tumorigenic dose of 3LL cells. As expected, no macro- or micro-tumor nodules were detected in the lungs in mice treated with saline or cDC (0/12, Fig. 3a). However, ~30% of mice injected with regDC developed lung tumors ( $p < 0.05$ ; Fig. 3a), which correlated with lower IFN- $\gamma$  production by splenic T cells stimulated with irradiated 3LL cells (Fig. 3b): CTL isolated from mice injected with regDC and developed tumors produced  $0.51 \pm 0.01$  pg/ml IFN- $\gamma$ , whereas IFN- $\gamma$  production by T cells isolated from saline- and cDC-treated groups secreted  $19.36 \pm 1.82$  and  $27.02 \pm 1.96$  pg/ml, respectively ( $p < 0.05$  between all groups). These data suggest that regDC exhibit a potent protumorigenic activity *in vivo*.

To confirm these results and evaluate the immunosuppressive potential of regDC *in vivo*, CD11c<sup>low</sup>CD11b<sup>high</sup> and CD11c<sup>high</sup>CD11b<sup>low</sup> DC subsets were injected in mice receiving the standard minimum tumorigenic dose of tumor cells. The results showed that mice injected with regDC developed significantly more macro- and micro-lung tumor nodules ( $p < 0.05$ , Fig. 3c) and significantly less tumor-specific IFN- $\gamma$  producing CTL in the spleens ( $p < 0.05$ ) when compared with two other groups of animals (Fig. 3d). For instance, the number of visual tumor nodules were  $13 \pm 3$ ,  $9 \pm 4$  and  $22 \pm 2$  in mice receiving saline, cDC and

regDC, respectively. Histological examination demonstrated that  $25 \pm 5$ ,  $20 \pm 4$  and  $75 \pm 8\%$  of tissue on the slide represented lung carcinoma in the same groups, respectively. Thus, regDC are potent inhibitors of the antitumor immunity *in vivo*.

Importantly, we did not observe upregulation of MDSC and Treg cells in lymphoid tissues after administration of regDC in 3LL-bearing mice (data not shown), suggesting independent immunosuppressive mechanisms of regDC in tumor-bearing mice. Together, these results raise a question about the mechanisms of  $\text{Cdc} \rightarrow \text{regDC}$  polarization and an opportunity to harness this process.

### Regulation of tumor-induced formation of regDC by small Rho GTPases and microtubule-targeting agents

We and others have recently reported that the key functions of DC, such as endocytosis, antigen processing/presentation and motility, are regulated by the small Rho GTPase family members, including Cdc42, Rac1/2 and RhoA,<sup>17–19</sup> whose activity could be modulated by different tumors.<sup>20</sup> Therefore, we tested the involvement of small Rho GTPases in  $\text{cDC} \rightarrow \text{regDC}$  polarization. As shown in Figure 4a, tumor cells caused significant redistribution of Cdc42 protein in DC downregulating its levels in the membrane fraction (active cell membrane-bound form) up to sevenfold ( $p < 0.05$ ) and upregulating it in a cytosol (inactive form of Rho GTPases) up to threefold ( $p < 0.05$ ). To confirm the specificity of 3LL effects on Cdc42 in DC, we used toxin B, a Rho GTPase inhibitor, and showed a similarity of 3LL and toxin B effects on Cdc42 redistribution in DC (Fig. 4a). These results suggested that small Rho GTPases may be involved in  $\text{cDC} \rightarrow \text{regDC}$  polarization in the tumor environment. But this suggestion required a confirmative demonstration that  $\text{cDC}$  polarization could be prevented by a small Rho GTPase activator.

However, there are no commercially available activators of Rho GTPases that can be used to reverse Rho GTPase inhibition in tumor-treated DC. As the Rho family of GTPases has been shown to regulate many aspects of intracellular actin cytoskeletal dynamics,<sup>21</sup> we hypothesized that certain microtubule-binding pharmacological agents might be useful for controlling DC polarization in the tumor environment. For instance, the microtubule-stabilizing drug paclitaxel (Taxol) is an FDA-approved antineoplastic cytotoxic agent. Recently, we have demonstrated that paclitaxel, when used in ultralow (nM) noncytotoxic noncytostatic concentrations, regulates classical and nonclassical Rho GTPases in DC<sup>22</sup> and upregulates DC maturation.<sup>23</sup> Importantly, the DC-potentiating effect of paclitaxel was blocked by a Rho GTPase inhibitor toxin B. Therefore, we evaluated if paclitaxel in low noncytotoxic concentrations affected regDC formation in our *in vitro* model system. Bone marrow-derived cDC were polarized by 3LL cells into regDC as above but with the addition of 1 nM paclitaxel. The appearance of immunosuppressive  $\text{CD11c}^{\text{low}}\text{CD11b}^{\text{high}}$  regDC was assessed by flow cytometry and confirmed functionally by their ability to inhibit proliferation of T cells. As expected, 3LL induced formation of regDC, increasing their levels up to fivefold among all  $\text{CD11c}^{\text{+}}$  cells ( $p < 0.05$ , Fig. 4c). These regDC exhibited a strong immunosuppressive potential with preactivated T cells, decreasing their proliferation by  $59.8 \pm 6.1\%$  ( $p < 0.05$ , Fig. 4b). However, 1 nM paclitaxel blocked regDC formation, decreasing their appearance in 3LL-treated DC cultures by twofold ( $p < 0.05$ , Fig. 4c). A

functional assay confirmed these results, showing that, unlike DC treated with 3LL, DC treated with 3LL in the presence of paclitaxel were unable to suppress T cell proliferation ( $p < 0.05$ , Fig. 4b). Importantly, the blocking effect of paclitaxel on regDC formation was prevented by a small Rho GTPase inhibitor toxin B (Figs. 4b and 4c). Thus, paclitaxel in noncytotoxic concentrations prevented tumor-induced polarization of cDC into regDC via the small Rho GTPase-mediated pathway, since the effect of paclitaxel was completely blocked by toxin B. These *in vitro* results raise a question about the ability of paclitaxel to control DC polarization *in vivo* and thus prevent emergence and accumulation of regDC in the tumor microenvironment *in vivo*.

### Regulation of regDC by ultralow noncytotoxic dose of paclitaxel *in vivo*

To determine the effect of paclitaxel on regDC *in vivo*, we first established noncytotoxic doses of the drug in mice bearing s.c. tumors. The results revealed that administration of 1/15-1/20 of maximum tolerated dose (MTD) of the drug showed no visible cytotoxicity in animals. For instance, Figure 5a shows that 1 mg/kg paclitaxel (1/20 MTD), in contrast to 15 mg/kg (~3/4 MTD), did not induce apoptotic cell death in the tumor mass 48 hr after a single administration, based on TUNEL staining. Similarly, 1 mg/kg paclitaxel, in contrast to 15 mg/kg, did not decrease the level of Ki67<sup>+</sup> cells on the same slides (data not shown), suggesting that this dose of paclitaxel is not cytostatic. Examination of mouse organs for gross lesions at necropsy after 5 weekly administrations of ultralow dose paclitaxel (1 mg/kg) revealed no general toxicity of the treatment.

Next, we tested if administration of paclitaxel (1 mg/kg i.p.) at D5 and D10 after i.v. inoculation of 3LL cells could affect formation of CD11c<sup>low</sup>CD11b<sup>high</sup> regDC in tumor-bearing mice seen at D14 (as in Fig. 1a). As expected, tumor progression was associated with significant upregulation of CD11c<sup>low</sup>CD11b<sup>high</sup> regDC (up to 9- to 10-fold,  $p < 0.05$ ) and decrease of CD11c<sup>high</sup>CD11b<sup>low</sup> cDC in the lungs and spleens. However, administration of ultralow, noncytotoxic doses of paclitaxel significantly abrogated tumor-induced increase in regDC and decrease in cDC. A representative example of data is shown in Figure 5b and demonstrates that, in the lungs of 3LL-bearing mice, paclitaxel abrogated a tenfold increase in regDC in more than a half and doubled the level of cDC. These results were reproduced in four independent studies and the summary of these data is shown in Figure 5c. As can be seen, paclitaxel significantly abrogated upregulation of regDC and downregulation of cDC in both the spleens and lungs in tumor-bearing mice ( $p < 0.05$ ). For example, based on the percentage of CD11c<sup>low</sup>CD11b<sup>high</sup> regDC among the total CD11c<sup>+</sup> cells in the spleens, paclitaxel completely blocked the twofold increase in regDC ( $p < 0.05$ ; left panel) and decreased the fivefold decline of cDC in half ( $p < 0.05$ ; right panel). Similar data were obtained for DC alterations in the lungs (Fig. 5c).

Next, we asked if the effect of paclitaxel on regDC emergence in 3LL-bearing mice could be mediated by the TLR4 signaling. This question arose from early published data showing that paclitaxel in subtherapeutic doses mimicked the action of TLR agonist LPS and induced maturation of mouse macrophages and DC.<sup>24,25</sup> Using TLR4-deficient mice and the same experimental design as above, we demonstrated that paclitaxel in ultralow dose prevented regDC formation by a TLR4-independent mechanism. The effect of paclitaxel on the



prevention of regDC accumulation in the 3LL environment in TLR4<sup>-/-</sup> mice was similar to its effect in WT animals (Fig. 5d). Thus, our results demonstrate that paclitaxel blocked tumor-induced formation of regDC *in vivo* and that its effect was not mediated by TLR4-mediated signaling.

### Paclitaxel-induced elimination of regDC increases the antitumor efficacy of DC vaccine

As the tumor-mediated emergence of protumorigenic regDC could be prevented by the ultralow dose of paclitaxel *in vivo*, the next question was whether paclitaxel could not only alter the tumor immunoenvironment, but also affect tumor progression in the 3LL model. Pilot experiments revealed that 2–4 biweekly administrations of ultralow dose paclitaxel did not significantly alter tumor formation in the lungs, despite marked downregulation of regDC levels. This is in agreement with studies showing that depletion of immune suppressor cells (*e.g.*, MDSC) alone does not efficiently inhibit tumor growth unless combined with other therapies.<sup>26–29</sup> The fact that resident DC differentiated from hematopoietic precursors in the tumor environment are functionally deficient<sup>8</sup> might explain this effect: even when paclitaxel prevented formation of immunosuppressive regDC in tumor-bearing mice, functionally deficient resident DC were unable to induce the efficient antitumor immunity. We thus tested if administration of functional exogenous DC in paclitaxel-treated 3LLbearing mice might improve the efficacy of regDC-blocking treatment. We added *ex vivo*-generated bone marrow-derived DC to the treatment protocol and used the following treatment procedure. Mice bearing 3LL tumor received 1 mg/kg paclitaxel i.p. on D6, D11 and D16 to prevent the regDC formation (group 2). To replace nonfunctional resident cDC, animals were inoculated i.p. with nonpulsed bone marrow-derived DC on D12 and D17 (group 3). A fourth group of mice received both paclitaxel and DC vaccine. Control tumor-bearing mice received saline (group 1).

As expected, paclitaxel and DC vaccine alone did not significantly abrogate formation of lung tumor nodules (Figs. 6a and 6b). However, the combination of ultralow-dose paclitaxel with DC vaccine resulted in inhibition of lung cancer development that exceeded that of either treatment alone. For instance, total lung weight was  $922 \pm 57$ ,  $884 \pm 49$ ,  $830 \pm 63$  and  $244 \pm 33$  mg in control, paclitaxel, DC and paclitaxel/DC groups, respectively ( $p < 0.05$  for paclitaxel/DC group *vs.* other groups, ANOVA); the number of visual macronodules was  $16 \pm 4$ ,  $14 \pm 4$ ,  $13 \pm 5$  and  $5 \pm 3$  for the same groups, respectively ( $p < 0.05$ , ANOVA, Fig. 6a). These results were confirmed by pathohistological examination of the lung tissues, demonstrating the similar levels of micrometastasis formation in control, paclitaxel and DC groups. Although the tumor nodules were of different size, they collectively comprised  $35 \pm 5$ ,  $32 \pm 5$  and  $30 \pm 6\%$  of tissue on the slides, respectively (Fig. 6b). However, treatment with paclitaxel + DC caused the appearance of significantly lower tumor nodules than in other groups, resulting in a three- to fourfold decrease in their collective area on tissue slides ( $8 \pm 5\%$ ,  $p < 0.05$ , ANOVA). Furthermore, this effect of combination treatment was associated with significant (up to 9- fold) increase in tumor-specific IFN- $\gamma$ -producing CTL. Finally, the survival of mice treated with a paclitaxel/DC combination was significantly longer than that of mice in the other groups with about ~30% of mice being tumor-free or having only 1–2 small nodules in the lungs on D50 (Fig. 6c). Thus, these results provide the

proof-of-principle that use of ultralow dose paclitaxel to prevent regDC formation in the tumor environment can support the antitumor effect of DC vaccine.

Seeking additional direct support for the significance of regDC targeting *in vivo* during tumor growth, and to investigate the contribution of CD11c<sup>+</sup>regDC to lung cancer progression, we used CD11c-DTR transgenic mice. In this strain, CD11c<sup>+</sup>DC express the receptor of diphtheria toxin (DT) and can be transiently depleted (>92%) by DT administration, whereas DT administration has no effect on CD11c<sup>+</sup> cells in WT mice.<sup>30</sup> ITgax-DTR/EGFP mice bearing 5-day-old i.v. 3LL tumors were treated with either PBS (control), paclitaxel+DC (×2) or i.p. DT 2 days prior to DC vaccine (×2). First, we confirmed the antitumor efficacy of the paclitaxel + DC combination in transgenic mice (Fig. 6d). Most importantly, the ablation of CD11c<sup>+</sup>DC after tumor injection and prior to DC replacement therapy resulted in similar significant inhibition of tumor growth in treated mice, with ~30% of mice remaining tumor-free in 50 days ( $p < 0.05$ , ANOVA and Wilcoxon's test) (Fig. 6d): lung weight was  $952 \pm 64$ ,  $282 \pm 46$  and  $268 \pm 38$  mg and number of lung nodules was  $18 \pm 6$ ,  $7 \pm 3$  and  $4 \pm 2$  in control (no treatment), paclitaxel + DC and DT + DC groups, respectively ( $p < 0.05$  for control vs. paclitaxel + DC or DT + DC;  $p > 0.05$  for paclitaxel + DC vs. DT + DC for both measurements, ANOVA).

Histopathological examination of lung specimens confirmed these results. Furthermore, elimination of regDC by either paclitaxel or DT-induced depletion of CD11c + DC (presumably, functionally deficient cDC and immunosuppressive regDC) in tumor-bearing mice evenly augmented the antitumor efficacy of DC replacement therapy in the 3LL-bearing mice. For example, evaluation of tumor-specific CTL in control and treated mice revealed that splenic T cells from tumor-bearing mice treated with paclitaxel plus DC vaccine, and DT plus DC vaccine, produced, respectively,  $254.14 \pm 15.95$  and  $242.05 \pm 15.31$  pg/ml IFN- $\gamma$  on stimulation with irradiated 3LL cells. IFN- $\gamma$  production by cells isolated from un-treated 3LL-bearers was  $17.93 \pm 1.42$  pg/ml ( $p < 0.05$ , ANOVA, Fig. 6e). These results demonstrated that either prevention of regDC formation by paclitaxel or their depletion with DT significantly enhanced the antitumor efficacy of DC-based therapy.

Altogether, our results show that resident regDC play an important role in supporting tumor progression in 3LL tumor model, but can be efficiently blocked by ultra low dose of paclitaxel, which prevents polarization of cDC into regDC by activating the small Rho GTPase signaling independently of TLR4.

## Discussion

It is now evident that the immunoregulatory cell network plays a major role in the failure of antitumor immune responses and immuno- and chemoimmunotherapies to eradicate tumors.<sup>31</sup> Immune regulatory cells can stimulate tumor growth, spreading and metastasis and suppress the activity of antitumor effector cells, suggesting that their elimination may inhibit tumor progression and augment the efficacy of anticancer therapies.<sup>32,33</sup> The protumorigenic role of several subpopulations of immune regulatory cells, *e.g.*, myeloid regulatory cells (MRC), including MDSC, TAM and N2 PMN, as well as Tregs, has been well demonstrated.<sup>11,28,34-39</sup>

DC are well characterized as potent antigen-presenting cells that initiate and maintain antitumor immunity. Numerous reports have demonstrated that the generation, function and survival of DC are compromised in the tumor microenvironment, suggesting that this is one of the key mechanisms of tumor escape from immune recognition.<sup>9</sup> Recently, it became evident that, in certain conditions, DC may provoke T cell tolerance and immune unresponsiveness. Although the emergence of regDC in the tumor environment has been recently suggested, their origin and the mechanisms of how cDC develop immunosuppressive properties remain unknown. Furthermore, pharmacological prevention of regDC recruitment and its therapeutic potential has been never tested.

Here, we have identified a new subset of MRC, regDC, which markedly increased the development of lung carcinoma by supporting tumor growth and inhibiting antitumor immune response. Previously, we and others have shown that the generation of murine and human DC from their precursors in the *in vitro* and *in vivo* tumor microenvironment results in unbalanced differentiation of DC precursors and accumulation of DC subsets with low expression of CD80, CD86, CD40, and MHC II and low IL-12 production.<sup>40–47</sup> Functionally, those DC were unable to stimulate T cell proliferation, failed to process and present model antigens and displayed decreased motility and endocytic activity. Collectively, these data led to the conclusion that resident DC differentiated from DC precursors in the tumor microenvironment are functionally impaired and thus unable to induce an adequate antitumor response. Liu *et al.*<sup>48</sup> have recently described the presence of CD11c<sup>low</sup>CD11b<sup>high</sup>Ia<sup>low</sup> immunosuppressive DC in s.c.-growing 3LL tumor. However, neither dynamics of regDC emergence *in vivo*, nor their presence in the orthotopic tumor microenvironment was tested yet.

First, we showed that the development of 3LL tumor in the lungs was associated with rapid accumulation of phenotypic regDC prior to the appearance of MDSC and Tregs (Fig. 1 and Supporting Information Table 1). Analysis of the phenotype of regDC revealed them to be CD103<sup>+</sup>CD205<sup>+/low</sup>CD11c<sup>low</sup>CD11b<sup>high/med</sup>CD80<sup>low</sup>CD86<sup>low</sup>MHC-II<sup>low</sup>PDCA1<sup>neg</sup> *Foxo3*<sup>neg</sup>F4/80<sup>neg</sup> cells. This is consistent with recent findings describing tumor-induced regDC as CD11b<sup>high</sup>Ia<sup>low</sup> cells inhibiting CD4<sup>+</sup> T cell responses.<sup>48</sup> To determine the origin of regDC in the tumor microenvironment, we sorted CD11c<sup>high</sup>CD11b<sup>neg</sup>GR-1<sup>neg</sup> cDC and CD11b<sup>+</sup>Gr-1<sup>+</sup>MDSC from the lungs of tumor-free mice and cultured them in tumor-conditioned medium. Flow cytometry analysis revealed the appearance of functional regDC (Fig. 2), suggesting that cDC and MDSC could polarize into regDC in the tumor environment. This explains the presence of both GR-1<sup>+</sup> and GR-1<sup>neg</sup> regDC subpopulations *in vivo*.

Furthermore, the biological significance of regDC was demonstrated in the *in vivo* models where the administration of regDC significantly upregulated formation of tumor nodules in the lungs, which was associated with inhibition of tumor-specific immune response (Fig. 3). We have also demonstrated that cDC → regDC polarization is mediated by small Rho GTPases. Interestingly, we have recently revealed the involvement of STAT3 activation in this process. Additional studies to determine if STAT3 is downstream or upstream of Rho GTPase signaling are in progress in our laboratory.

A better understanding of the events that allow cDC → regDC polarization can provide insight into the contribution of regDC to cancer development and promote the design of therapies that control accumulation and function of regDC. In fact, we revealed that paclitaxel could block regDC formation both *in vitro* and *in vivo* (Figs. 4 and 5). We have also shown that blockage of regDC formation by paclitaxel significantly augmented development of the antitumor immune response induced by DC replacement therapy and resulted in significant inhibition of tumor growth.

In summary, our data show that tumor-induced regDC represent important contributors to tumor growth in at least some types of cancer. Therefore, understanding the role of regDC in different tumor models and development of specific targeted therapies to prevent polarization of cDC and MDSC into regDC will open new opportunities to decrease the immunosuppressive and protumorigenic potential of the tumor immunoenvironment and, in turn, increase the efficacy of anticancer therapies.

## Supplementary Material

Refer to Web version on PubMed Central for supplementary material.

## Acknowledgments

This work was supported by RO1 CA154369 from NCI, NIH (to Michael R. Shurin) and Nature Science Foundation of China 81101722 (to Hua Zhong)

## References

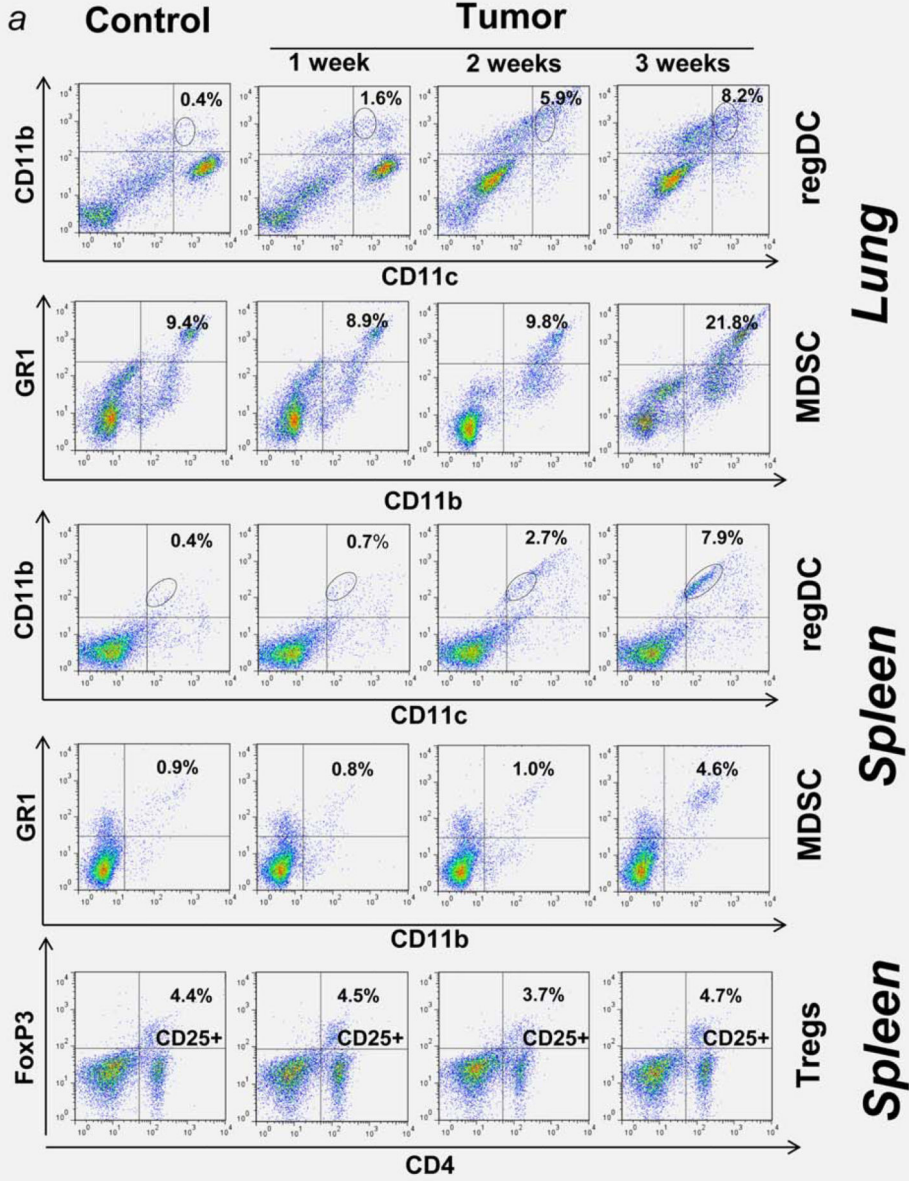
1. Kidd S, Spaeth E, Watson K, et al. Origins of the tumor microenvironment: quantitative assessment of adipose-derived and bone marrow-derived stroma. *PLoS One*. 2012; 7:e30563. [PubMed: 22363446]
2. Tarin D. Clinical and biological implications of the tumor microenvironment. *Cancer Microenviron*. 2012; 5:95–112. [PubMed: 22782446]
3. Correia AL, Bissell MJ. The tumor microenvironment is a dominant force in multidrug resistance. *Drug Resist Update*. 2012; 15:39–49.
4. Swartz MA, Iida N, Roberts EW, et al. Tumor microenvironment complexity: emerging roles in cancer therapy. *Cancer Res*. 2012; 72:2473–2480. [PubMed: 22414581]
5. Spano D, Zollo M. Tumor microenvironment: a main actor in the metastasis process. *Clin Exp Metastasis*. 2012; 29:381–395. [PubMed: 22322279]
6. Biragyn A, Longo DL. Neoplastic "Black Ops": cancer's subversive tactics in overcoming host defenses. *Semin Cancer Biol*. 2012; 22:50–59. [PubMed: 22257681]
7. Hanahan D, Coussens LM. Accessories to the crime: functions of cells recruited to the tumor microenvironment. *Cancer Cell*. 2012; 21:309–322. [PubMed: 22439926]
8. Gabrilovich DI, Ostrand-Rosenberg S, Bronte V. Coordinated regulation of myeloid cells by tumours. *Nat Rev Immunol*. 2012; 12:253–268. [PubMed: 22437938]
9. Ma Y, Shurin GV, Gutkin DW, Shurin MR. Tumor associated regulatory dendritic cells. *Semin Cancer Biol*. 2012; 22:298–306. [PubMed: 22414911]
10. Manicassamy S, Pulendran B. Dendritic cell control of tolerogenic responses. *Immunol Rev*. 2011; 241:206–227. [PubMed: 21488899]
11. Shurin MR, Naiditch H, Zhong H, et al. Regulatory dendritic cells: new targets for cancer immunotherapy. *Cancer Biol Ther*. 2011; 11:988–992. [PubMed: 21474998]
12. Lande R, Gilliet M. Plasmacytoid dendritic cells: key players in the initiation and regulation of immune responses. *Ann N Y Acad Sci*. 2010; 1183:89–103. [PubMed: 20146710]

13. Hurwitz AA, Watkins SK. Immune suppression in the tumor microenvironment: a role for dendritic cell-mediated tolerization of T cells. *Cancer Immunol Immunother.* 2012; 61:289–293. [PubMed: 22237887]
14. Norian LA, Rodriguez PC, O'Mara LA, et al. Tumor-infiltrating regulatory dendritic cells inhibit CD81 T cell function via L-arginine metabolism. *Cancer Res.* 2009; 69:3086–3094. [PubMed: 19293186]
15. Fu BM, He XS, Yu S, et al. A tolerogenic semi-mature dendritic cells induce effector T-cell hyporesponsiveness by activation of antigen-specific CD4+CD25+ T regulatory cells that promotes skin allograft survival in mice. *Cell Immunol.* 2010; 261:69–76. [PubMed: 20038461]
16. Watkins SK, Zhu Z, Riboldi E, et al. FOXO3 programs tumor-associated DCs to become tolerogenic in human and murine prostate cancer. *J Clin Invest.* 2011; 121:1361–1372. [PubMed: 21436588]
17. Kerksiek KM, Niedergang F, Chavrier P, et al. Selective Rac1 inhibition in dendritic cells diminishes apoptotic cell uptake and cross-presentation in vivo. *Blood.* 2005; 105:742–749. [PubMed: 15383465]
18. Kobayashi M, Azuma E, Ido M, et al. A pivotal role of Rho GTPase in the regulation of morphology and function of dendritic cells. *J Immunol.* 2001; 167:3585–3591. [PubMed: 11564770]
19. Shurin GV, Tourkova IL, Chatta GS, et al. Small rho GTPases regulate antigen presentation in dendritic cells. *J Immunol.* 2005; 174:3394–3400. [PubMed: 15749872]
20. Tourkova IL, Shurin GV, Wei S, et al. Small rho GTPases mediate tumor-induced inhibition of endocytic activity of dendritic cells. *J Immunol.* 2007; 178:7787–7793. [PubMed: 17548616]
21. Spiering D, Hodgson L. Dynamics of the Rho family small GTPases in actin regulation and motility. *Cell Adh Migr.* 2011; 5:170–180. [PubMed: 21178402]
22. Shurin GV, Tourkova IL, Shurin MR. Low-dose chemotherapeutic agents regulate small Rho GTPase activity in dendritic cells. *J Immunother.* 2008; 31:491–499. [PubMed: 18463535]
23. Shurin GV, Tourkova IL, Kaneno R, et al. Chemotherapeutic agents in noncytotoxic concentrations increase antigen presentation by dendritic cells via an IL-12-dependent mechanism. *J Immunol.* 2009; 183:137–144. [PubMed: 19535620]
24. Chan OT, Yang LX. The immunological effects of taxanes. *Cancer Immunol Immunother.* 2000; 49:181–185. [PubMed: 10941900]
25. Pfannenstiel LW, Lam SS, Emens LA, et al. Paclitaxel enhances early dendritic cell maturation and function through TLR4 signaling in mice. *Cell Immunol.* 2010; 263:79–87. [PubMed: 20346445]
26. Yang L, Carbone DP. Tumor–host immune interactions and dendritic cell dysfunction. *Adv Cancer Res.* 2004; 92:13–27. [PubMed: 15530555]
27. Suzuki E, Kapoor V, Jassar AS, et al. Gemcitabine selectively eliminates splenic Gr-1+/CD11b+ myeloid suppressor cells in tumor-bearing animals and enhances antitumor immune activity. *Clin Cancer Res.* 2005; 11:6713–6721. [PubMed: 16166452]
28. Gabrilovich DI, Nagaraj S. Myeloid-derived suppressor cells as regulators of the immune system. *Nat Rev Immunol.* 2009; 9:162–174. [PubMed: 19197294]
29. Ozao-Choy J, Ma G, Kao J, et al. The novel role of tyrosine kinase inhibitor in the reversal of immune suppression and modulation of tumor microenvironment for immune-based cancer therapies. *Cancer Res.* 2009; 69:2514–2522. [PubMed: 19276342]
30. Huarte E, Cubillos-Ruiz JR, Nesbeth YC, et al. Depletion of dendritic cells delays ovarian cancer progression by boosting antitumor immunity. *Cancer Res.* 2008; 68:7684–7691. [PubMed: 18768667]
31. Witz IP. The tumor microenvironment: the making of a paradigm. *Cancer Microenviron.* 2009; 2(Suppl 1):9–17. [PubMed: 19701697]
32. Shurin MR, Shurin GV, Lokshin A, et al. Intratumoral cytokines/chemokines/growth factors and tumor infiltrating dendritic cells: friends or enemies? *Cancer Metastasis Rev.* 2006; 25:333–356. [PubMed: 17029028]
33. Rabinovich GA, Gabrilovich D, Sotomayor EM. Immunosuppressive strategies that are mediated by tumor cells. *Annu Rev Immunol.* 2007; 25:267–296. [PubMed: 17134371]

34. Mantovani A, Sica A. Macrophages, innate immunity and cancer: balance, tolerance, and diversity. *Curr Opin Immunol.* 2010; 22:231–237. [PubMed: 20144856]
35. Younos I, Donkor M, Hoke T, et al. Tumor- and organ-dependent infiltration by myeloid-derived suppressor cells. *Int Immunopharmacol.* 2011; 11:816–826. [PubMed: 21376153]
36. Gregory AD, Houghton AM. Tumor-associated neutrophils: new targets for cancer therapy. *Cancer Res.* 2011; 71:2411–2416. [PubMed: 21427354]
37. Nagaraj S, Gabrilovich DI. Tumor escape mechanism governed by myeloid-derived suppressor cells. *Cancer Res.* 2008; 68:2561–2563. [PubMed: 18413722]
38. Ko JS, Bukowski RM, Fincke JH. Myeloid-derived suppressor cells: a novel therapeutic target. *Curr Oncol Rep.* 2009; 11:87–93. [PubMed: 19216839]
39. Ostrand-Rosenberg S, Sinha P. Myeloid-derived suppressor cells: linking inflammation and cancer. *J Immunol.* 2009; 182:4499–4506. [PubMed: 19342621]
40. Aalamian M, Pirskhalaishvili G, Nunez A, et al. Human prostate cancer regulates generation and maturation of monocyte-derived dendritic cells. *Prostate.* 2001; 46:68–75. [PubMed: 11170134]
41. Katsenelson NS, Shurin GV, Bykovskaia SN, et al. Human small cell lung carcinoma and carcinoid tumor regulate dendritic cell maturation and function. *Mod Pathol.* 2001; 14:40–45. [PubMed: 11211308]
42. Shurin GV, Aalamian M, Pirskhalaishvili G, et al. Human prostate cancer blocks the generation of dendritic cells from cd34+ hematopoietic progenitors. *Eur Urol.* 2001; 39(Suppl 4):37–40. [PubMed: 11340288]
43. Shurin GV, Shurin MR, Bykovskaia S, et al. Neuroblastoma-derived gangliosides inhibit dendritic cell generation and function. *Cancer Res.* 2001; 61:363–369. [PubMed: 11196188]
44. Shurin MR, Yurkovetsky ZR, Tourkova IL, et al. Inhibition of CD40 expression and CD40-mediated dendritic cell function by tumor-derived IL-10. *Int J Cancer.* 2002; 101:61–68. [PubMed: 12209589]
45. Song EY, Shurin MR, Tourkova IL, et al. Human renal cell carcinoma inhibits dendritic cell maturation and functions. *Urol A.* 2004; 43(Suppl 3):S128–S130.
46. Tourkova IL, Yamabe K, Foster B, et al. Murine prostate cancer inhibits both in vivo and in vitro generation of dendritic cells from bone marrow precursors. *Prostate.* 2004; 59:203–213. [PubMed: 15042620]
47. Aalamian-Matheis M, Chatta GS, et al. Inhibition of dendritic cell generation and function by serum from prostate cancer patients: correlation with serum-free PSA. *Adv Exp Med Biol.* 2007; 601:173–182. [PubMed: 17713004]
48. Liu Q, Zhang C, Sun A, et al. Tumor-educated CD11b<sup>high</sup>low regulatory dendritic cells suppress T cell response through arginase I. *J Immunol.* 2009; 182:6207–6216. [PubMed: 19414774]
49. Shurin MR, Pandharipande PP, Zorina TD, et al. FLT3 ligand induces the generation of functionally active dendritic cells in mice. *Cell Immunol.* 1997; 179:174–184. [PubMed: 9268501]

**What's new?**

Cells that suppress the immune response are known to be recruited to the tumor microenvironment, and most of these cell types are quite well understood. However, recent studies have indicated that dendritic cells (DCs) can play a similar role. In this study, the authors found that both conventional DCs and MDSCs may actually be reprogrammed by the tumor microenvironment into a tolerogenic state, becoming regulatory DCs (regDCs). They report the molecular mechanism by which this conversion occurs, and show that paclitaxel can prevent it. These results suggest that regDCs may represent a promising therapeutic target.





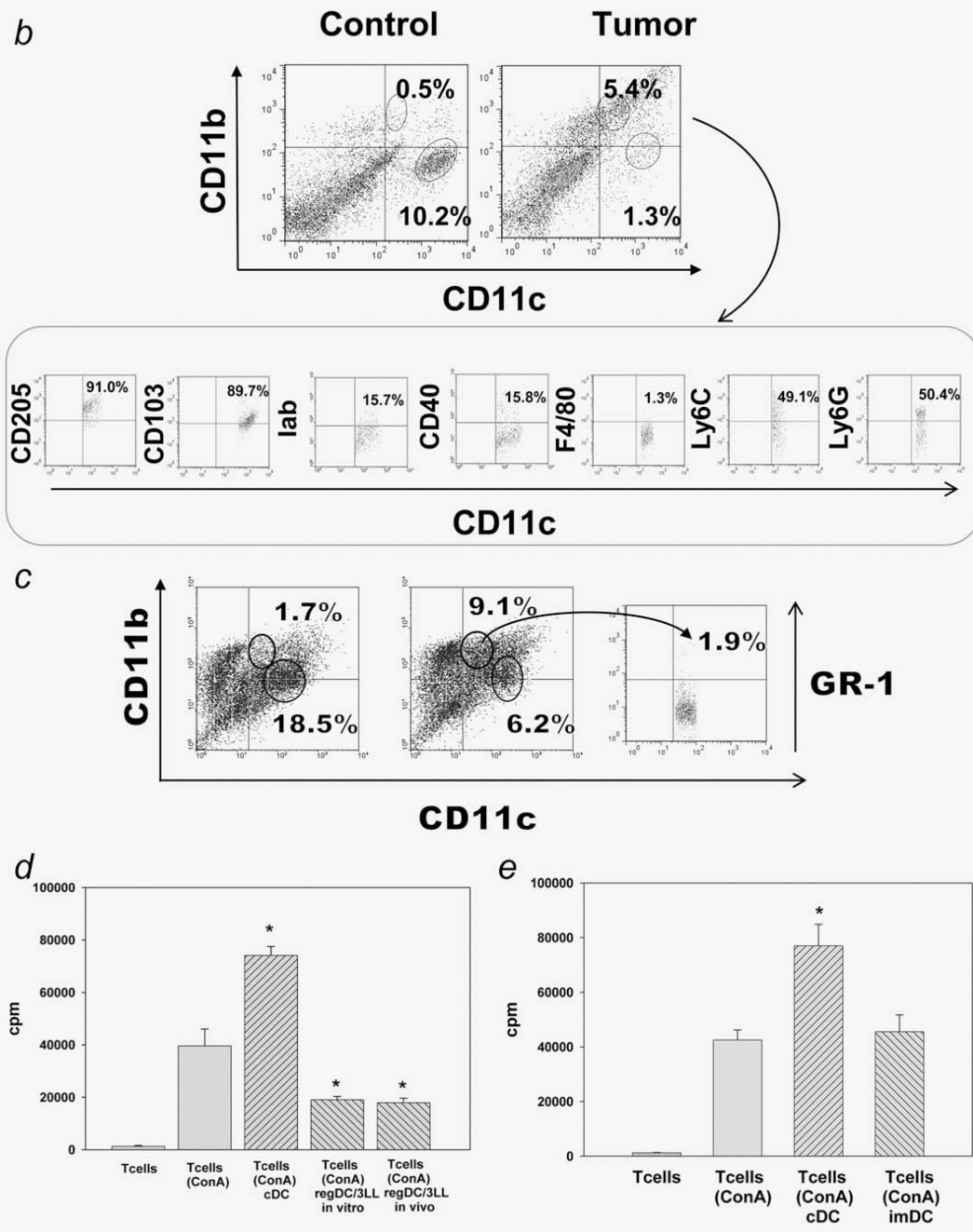
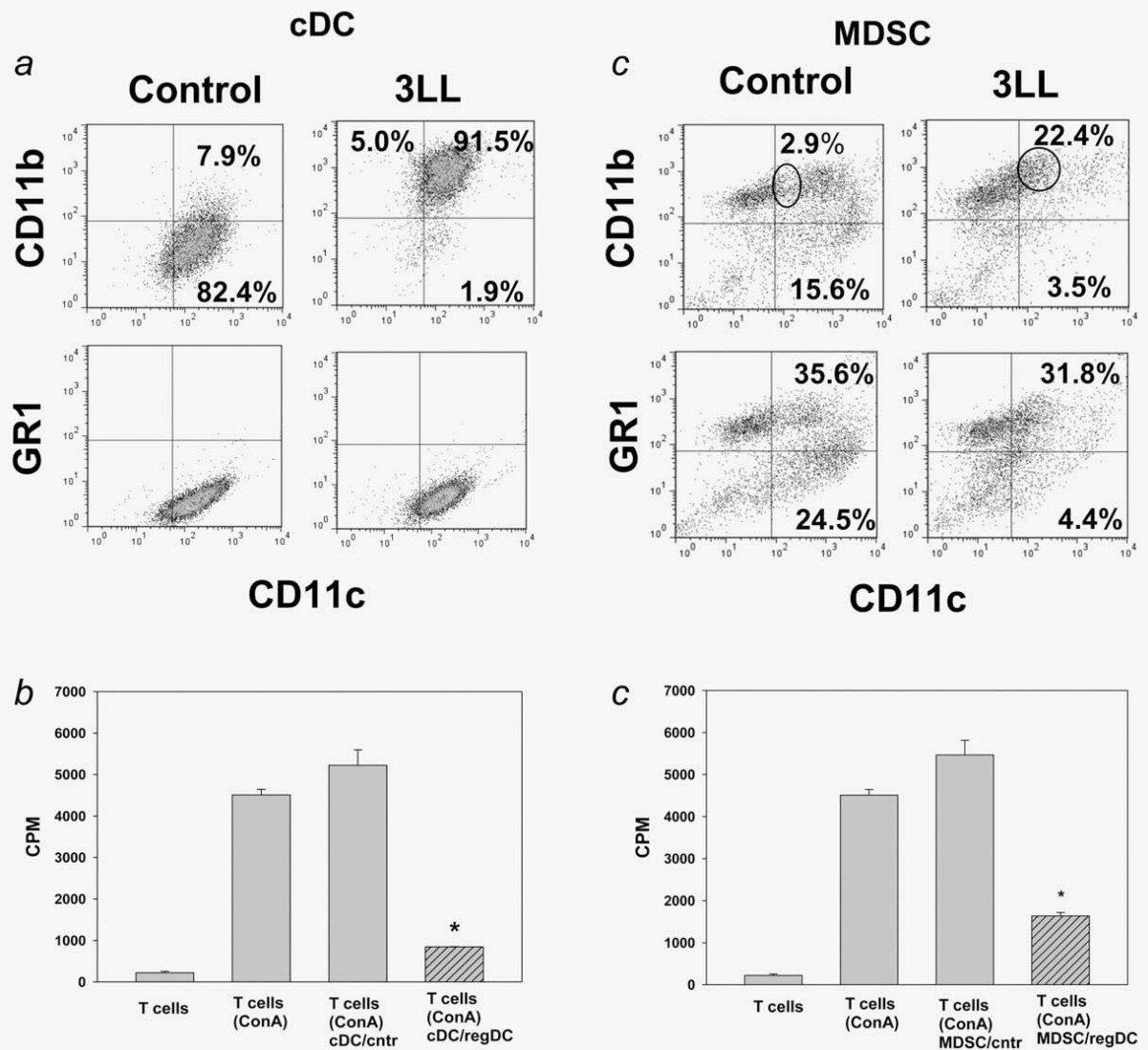


**Figure 1.**

Immune regulators in the lung cancer microenvironment. 3LL-induced polarization of cDC into immunosuppressive regDC in vivo. (a) Early emergence of regDC, but not MDSC or Treg cells, in the lung and spleen after tumor cell inoculation. Mice received 3LL cells and tissues were collected 7, 14 and 21 days later as described in M&M. Flow cytometry analysis of CD11c<sup>low</sup>CD11b<sup>high/med</sup> regDC, MDSC and Treg cells revealed appearance of regDC within the first week after tumor cell injection, while the levels of MDSC and Treg cells increased 2 weeks later. Data are shown as the percentage of positive cells from a

representative experiment ( $N=4-5$ ). (b) Low expression of co-stimulatory molecules on tumor-associated regDC. Lungs were harvested from tumor-free (left panel) and 3LL-bearing (right panel) mice. Single cell suspensions were subjected to flow cytometric analysis as described in M&M. Significant upregulation of CD11c<sup>low</sup>CD11b<sup>high</sup> regDC and downregulation of CD11c<sup>high</sup>CD11b<sup>low/neg</sup> cDC were seen in all experiments ( $N>10$ ). Data are shown as the percentage of positive cells from a representative experiment. (c) Polarization of bone marrow-derived cDC into immunosuppressive regDC in the lung cancer microenvironment *in vitro*. DC were generated from the bone marrow precursors and treated with 3LL-conditioned medium on Day 5 as described in M&M. Flow cytometry analysis revealed increased levels of regDC and decreased content of cDC subsets. The results are shown as the percentage of positive cells in a representative experiment. Similar data were obtained in seven independent studies. (d) Immunosuppressive activity of tumor-associated regDC. CD11c<sup>low</sup>CD11b<sup>high</sup> regDC were sorted from the lungs harvested 2 weeks after mice were injected with 3LL cells (regDC/3LL *in vivo*) or from the bone marrow-derived DC treated on Day 5 with 3LL-conditioned medium for 48 hr (regDC/3LL *in vitro*). Control CD11c<sup>high</sup>CD11b<sup>low/neg</sup> cDC were either bone marrow-derived cDC or lung cDC isolated from tumor-free mice (cDC). All DC subsets were added at the same ratio (1:100) to ConA-prestimulated syngeneic T cells. T cell proliferation was assessed by <sup>3</sup>H-thymidine incorporation and expressed as count per minute (cpm). Proliferation of intact T cells and ConA-stimulated T cells (w/o DC) is shown as white bars. \* $p < 0.05$  (ANOVA, mean  $\pm$  SEM,  $N = 5-6$ ). (e) Inability of immature DC (imDC) to suppress proliferation of T lymphocytes. Bone marrow-derived imDC and conventional cDC were generated as described in M&M. All DC subsets were added at the same ratio to ConA-prestimulated syngeneic T cells. T cell proliferation was assessed by <sup>3</sup>H-thymidine incorporation. Proliferation of intact T cells and ConA-stimulated T cells (w/o DC) is shown as white bars. \* $p < 0.05$  (ANOVA, mean  $\pm$  SEM,  $N = 3$ ).

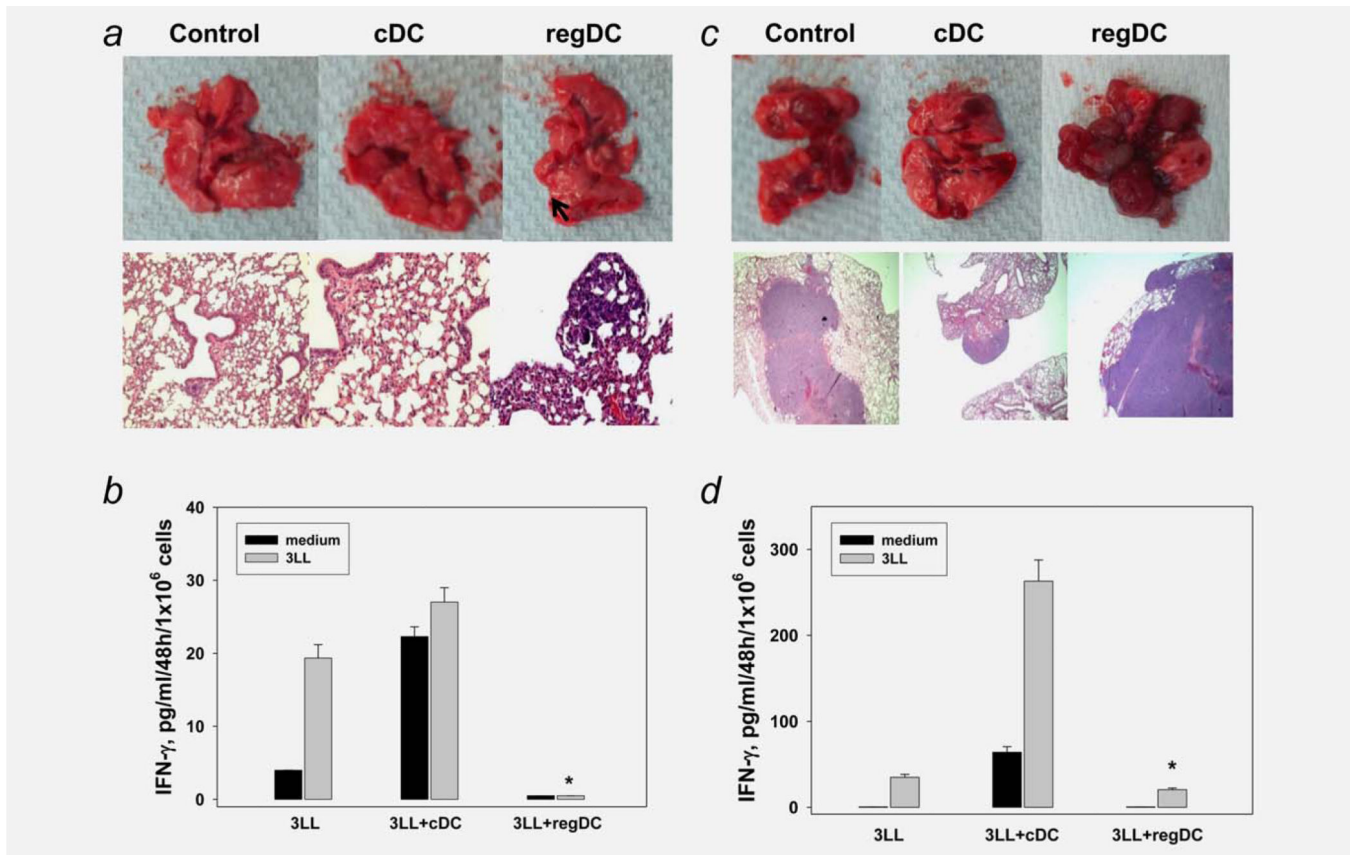
[Color figure can be viewed in the online issue, which is available at [wileyonlinelibrary.com](http://wileyonlinelibrary.com).]



**Figure 2.**

Tumor-induced polarization of cDC and MDSC into regDC *ex vivo*. (a) CD11c<sup>+</sup> cDC and MDSC were isolated by FACS cell sorting from the lungs of tumor-free mice and used for phenotypic and functional assays. (b) Polarization of cDC into regDC *ex vivo*. Lung CD11c<sup>+</sup> cDC were cultured *ex vivo* with 3LL cells in inserts for 72 hr. Flow cytometric analysis revealed the appearance of GR-1 negative regDC. The results are shown as the percentage of positive cells in a representative experiment with similar results obtained from four independent experiments. (c) Inhibition of T cell proliferation by cDC-derived regDC. Control lung CD11c<sup>+</sup>cDC or cDC-derived regDC were harvested and added at the same ratio (1:100) to ConA-prestimulated syngeneic T cells. T cell proliferation was assessed by <sup>3</sup>H-thymidine incorporation and expressed as count per minute (cpm). \**p* < 0.05 (ANOVA, mean ± SEM, *N* = 3). (d) Polarization of MDSC into regDC *ex vivo*. MDSC isolated from lung of tumor free mice were cultured *ex vivo* with 3LL cells in inserts for 72 hr. Tumor cells polarized lung MDSC into the regDC *ex vivo*. (e) Inhibition of T cell

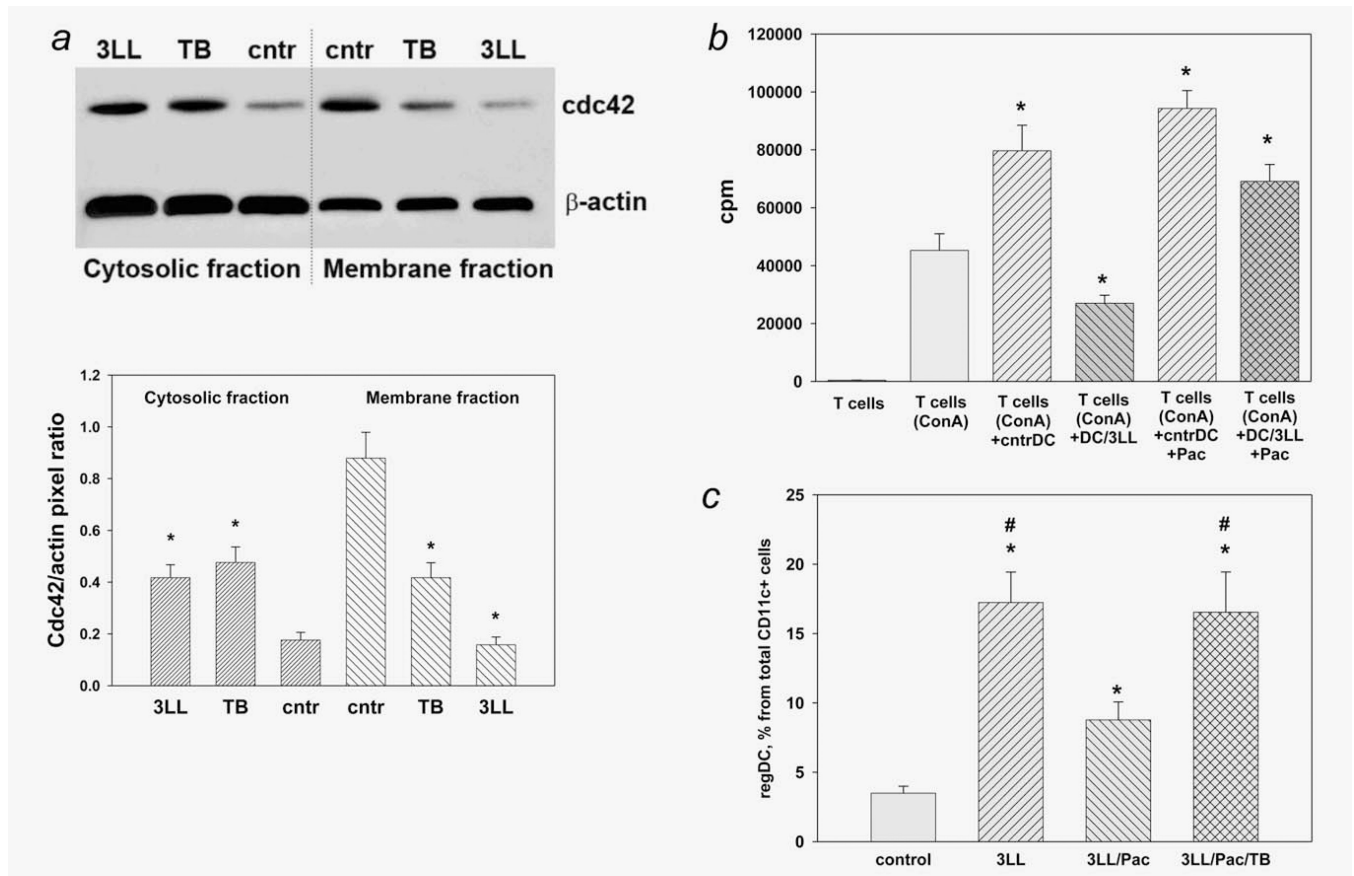
proliferation by MDSC-derived regDC. Tumor-induced regDC derived from MDSC were isolated by FACS cell sorting from the cell cultures and used in T cell proliferation assay as described in (c). MDSC-derived regDC significantly inhibited proliferation of preactivated T cells as compared to control untreated MDSC.  $*p < 0.05$  (ANOVA, mean  $\pm$  SEM,  $N = 3$ ).



**Figure 3.**

Regulatory DC support tumor growth and attenuate antitumor immunity. (a) Administration of regDC but not cDC induced tumor development in the lung. Sorted *in vitro* generated regDC and cDC were injected in mice on Days 3 and 10 after inoculation of 1/10 of the minimum tumorigenic dose of 3LL cells. Animals were sacrificed at Day 21 and the lungs were removed, fixed and subjected to H&E staining. Control animals received only 3LL cells. Upper panels: visual appearance of tumor nodules in the lungs after administration of regDC. Low panels: H&E staining of the lung tissues for visualization of micronodules of lung carcinoma. The results of a representative experiment are shown ( $N = 3$ ). (b) Inhibition of tumor-specific CTL by regDC *in vivo*. Splenic T lymphocytes were isolated from mice receiving either 1/10 minimum tumorigenic dose of tumor cells only (3LL), tumor cells and cDC (3LL + cDC) or tumor cells and regDC (3LL + regDC). Cells were stimulated with medium (black bars) or irradiated 3LL cells (gray bars). IFN- $\gamma$  levels in cell-free supernatants were assessed by ELISA. Data represent the mean  $\pm$  SEM from three independent experiments. \*  $p < 0.05$  vs. 3LL and 3LL + cDC groups (ANOVA). (c) Administration of regDC, but not cDC augmented tumor development in the lungs. Sorted regDC and cDC were injected in mice together with 3LL cells at the minimum tumorigenic dose and the lungs were harvested 3 weeks after tumor cell injection. Upper panels: visual appearance of tumor nodules in the lungs. Low panels: H&E staining of the lung tissues for histopathological visualization of micronodules of lung carcinoma ( $\times 100$ ). The results of a representative experiment are shown ( $N = 3$ ). (d) Inhibition of tumor-specific CTL by regDC

*in vivo*. Splenic T lymphocytes were isolated from mice receiving either tumor cells only (3LL), tumor cells and cDC (3LL + cDC) or tumor cells and regDC (3LL + regDC). Cells were stimulated with medium (black bars) or irradiated 3LL cells (gray bars). IFN- $\gamma$  levels in cell-free supernatants were assessed by ELISA. Data represent the mean  $\pm$  SEM from three independent experiments. \* $p$  < 0.05 vs. 3LL and 3LL + cDC groups (ANOVA).

**Figure 4.**

Regulation of tumor-induced formation of regDC by Rho GTPases and paclitaxel *in vitro*.

(a) Decrease in active (membrane) and increase in inactive (cytosolic) Cdc42 in 3LL-treated DC. Bone marrow-derived DC were treated with medium (cntr), small Rho GTPase inhibitor toxin B (TB) and 3LL conditioned medium (3LL). Active and nonactive Cdc42 was assessed as Cdc42 protein levels in the membrane and cytosolic fractions of DC, respectively, by Western blot analysis (upper panel) as described in M&M. The results of a representative experiment are shown ( $N = 3$ ). Densitometry was used for enumeration of the protein redistribution data (low panel). Data are shown as the mean  $\pm$  SEM of Cdc42 levels relative to  $\beta$ -actin levels in the same fractions. \* $p < 0.05$  vs. control (ANOVA,  $N = 3$ ). (b) Paclitaxel prevented 3LL-induced polarization of cDC into regDC *in vitro*. Bone marrow-derived cDC were polarized into regDC by the addition of 3LL conditioned medium (3LL) in the presence or absence of paclitaxel (Pac, 1 nM). Functional activity of medium-treated DC (cntrDC) and 3LL-treated cells (DC/3LL) was assessed by their ability to suppress proliferation of ConA-preactivated syngeneic T cells. T cell proliferation was determined by  $^3\text{H}$ -thymidine incorporation and expressed as count per minute (cpm). Proliferation of intact T cells and ConA-stimulated T cells (w/o DC) is shown as white bars. \* $p < 0.05$  vs. (T cells + Con A) group (ANOVA,  $N = 3$ , mean  $\pm$  SEM). (c) Toxin B reversed the ability of paclitaxel to prevent tumor-induced formation of regDC *in vitro*. Bone marrow-derived DC were treated with 3LL conditioned medium (3LL) alone or in the presence of paclitaxel (Pac, 1 nM) without or with toxin B (TB, 0.2 ng/ml). Appearance of regDC was assessed by

flow cytometry. Data from three independent experiments are shown as the mean  $\pm$  SEM. \* $p$  <0.05 vs. control DC (medium-treated); # $p$  <0.05 vs. 3LL/PAC group (ANOVA).



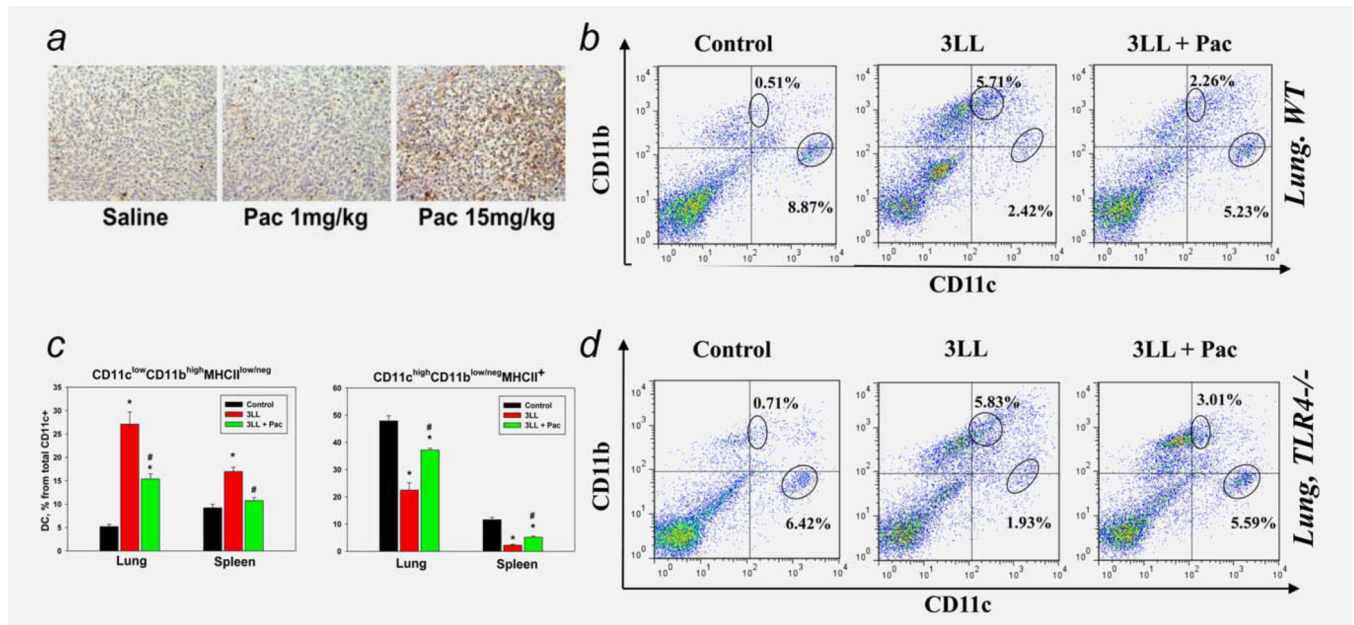


**Figure 5.**

Paclitaxel inhibited tumor-induced DC polarization *in vivo* in TLR4-independent manner. (a) Establishing of ultralow noncytotoxic doses of paclitaxel *in vivo*. Mice were inoculated s.c. with 3LL cells and when tumors reached ~20–25 mm<sup>2</sup>, mice were given i.p. saline or paclitaxel (Pac) at low (1 mg/kg i.p.) or three-fourth of standard maximum tolerated dose (MTD, 15 mg/kg). Tumors were harvested 48 hr later and analyzed for dead cells by TUNEL staining (brown). No apoptotic cells were detected when 1 mg/kg of paclitaxel was administered. Images from a representative experiment are shown ( $N = 3$ ). (b) Paclitaxel prevented tumor-induced downregulation of cDC and upregulation of regDC in the lung cancer microenvironment *in vivo*. Paclitaxel in low noncytotoxic dose (Pac, 1 mg/kg  $\times 2$ ) was administered in 3LL lung carcinoma-bearing mice (3LL). Lungs were harvested 2 weeks after tumor cell inoculation and analyzed for the distribution of CD11c<sup>high</sup>CD11b<sup>low/neg</sup> cDC and CD11c<sup>low</sup>CD11b<sup>high</sup> regDC subsets by flow cytometry. Tumor-free animals served as a control. Representative results from one out of five independent experiments are shown. (c) Paclitaxel prevented tumor-induced redistribution of cDC and regDC in lymphoid and nonlymphoid tissues *in vivo*. Paclitaxel in low noncytotoxic dose (Pac, 1 mg/kg  $\times 2$ ) was administered in 3LL lung carcinoma-bearing mice (3LL). Spleens and lungs were harvested 2 weeks after tumor cell inoculation and analyzed for the distribution of cDC and regDC subsets by flow cytometry. Tumor-free animals served as a control. The summary results from three independent experiments are shown. \* $p < 0.05$  vs. tumor-free mice; # $p < 0.05$  vs. nontreated 3LL-bearing mice (ANOVA,  $N = 3$ , mean  $\pm$  SEM). (d) Blockade of tumor-induced accumulation of regDC by paclitaxel *in vivo* was not mediated by the TLR4 signaling. Tumor-bearing wild type and TLR4 knockout mice were treated with ultralow dose of paclitaxel and analyzed as in (b). Representative results from one out of two independent experiments are shown.

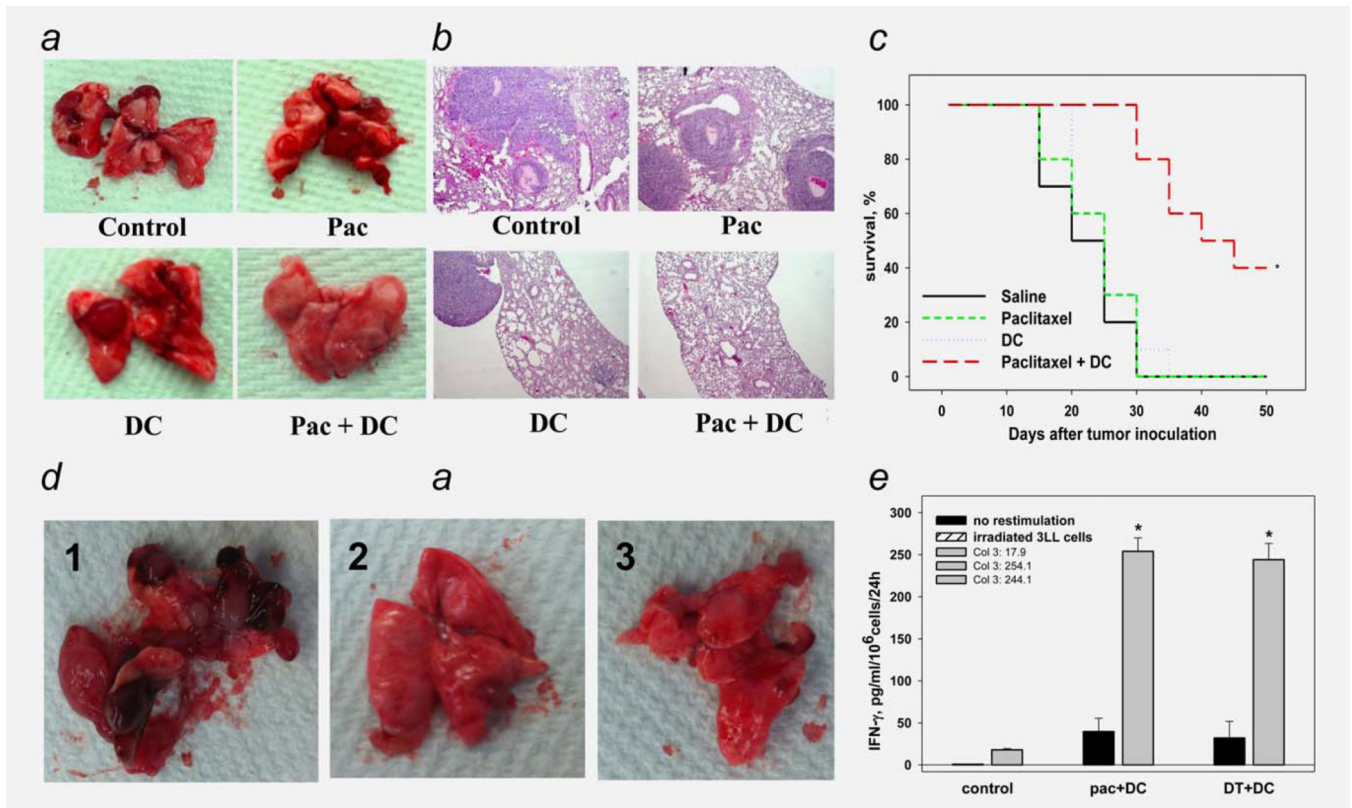


**Figure 6.**

Paclitaxel-induced elimination of regDC augmented the antitumor efficacy of DC vaccine. (a), (b) Blockage of regDC accumulation by ultra low dose paclitaxel improved the antitumor potential of DC administration in tumor-bearing mice. Mice-bearing i.v. administered 3LL tumor received 1 mg/kg paclitaxel i.p. on Days 6, 11 and 16 to prevent the regDC formation (“Pac” group) or were inoculated i.p. with nonpulsed bone marrow-derived DC on Days 12 and 17 (“DC” group). Other tumor-bearing mice received both treatments together (“Pac + DC” group) or were treated with saline (control). Lungs were harvested 3 weeks after tumor cell administration and analyzed for visual tumor nodules (a) or were fixed and stained with H&E for histopathological examination of microtumors ( $\times 100$ ) (b). The results from a representative experiments are shown ( $N = 3$ ). (c) Combination of ultra low dose paclitaxel and DC vaccine prolonged survival of mice with lung adenocarcinoma. Mice were treated as described in (a) and checked for survival in three independent experiments. The summary data are shown as the Kaplan–Meier survival curve.  $*p < 0.05$  (log-rank test). (d), (e) Elimination of regDC by either paclitaxel or depletion of CD11c + DC in tumor-bearing mice evenly augmented the antitumor efficacy of DC replacement therapy. CD11c-DTR transgenic mice bearing 5-Day old i.v. 3LL tumors were treated with either PBS (control, panel 1), paclitaxel + DC ( $\times 2$ ) (Pac + DC, panel 2) or i.p. DT 2 days prior to DC vaccine (DT+ DC, panel 3). Lungs were harvested 3 weeks after tumor cell administration and analyzed for visual tumor nodules (d). (e) Splenic T lymphocytes were isolated from the same mice stimulated with medium (black bars) or irradiated 3LL cells

(gray bars). IFN- $\gamma$  levels in cell-free supernatants were assessed by ELISA. Data represent the mean  $\pm$  SEM from three independent experiments. \* $p$  < 0.05 vs. control (ANOVA).